Biochemistry and Biophysics Reports 30 (2022) 101257

Contents lists available at ScienceDirect

Biochemistry and Biophysics Reports

journal homepage: www.elsevier.com/locate/bbrep

The involvement of oxysterol-binding protein related protein (ORP) 6 in the counter-transport of phosphatidylinositol-4-phosphate (PI4P) and phosphatidylserine (PS) in neurons

Shinya Mochizuki, Harukata Miki, Ruyun Zhou, Yasuko Noda *

Dept. of Anatomy, Bioimaging and Neuro-cell Science, Jichi Medical University, Japan

ARTICLE INFO

Keywords:
Oxysterol
ORP6
Membrane contact site
Oxysterol-binding protein
PI4P
PS
Counter-transport

ABSTRACT

Oxysterol-binding protein (OSBP)-related protein (ORP) 6, a member of subfamily III in the ORP family, localizes to membrane contact sites between the endoplasmic reticulum (ER) and other organelles and functions in non-vesicular exchange of lipids including phosphatidylinositol-4-phosphate (PI4P) in neurons. In this study, we searched for the lipid counter-transported in exchange for PI4P by using molecular cell biology techniques. Deconvolution microscopy revealed that knockdown of ORP6 partially shifted localization of a phosphatidylserine (PS) marker but not filipin in primary cultured cerebellar neurons. Overexpression of ORP6 constructs lacking the OSBP-related ligand binding domain (ORD) resulted in the same shift of the PS marker. A PI4KIIIα inhibitor specifically inhibiting the synthesis and plasma membrane (PM) localization of PI4P, suppressed the localization of ORP6 and the PS marker at the PM. Overexpression of mutant PS synthase 1 (PSS1) inhibited transport of the PS marker to the PM and relocated the PI4P marker to the PM in Neuro-2A cells. Introduction of ORP6 but not the dominant negative ORP6 constructs, shifted the localization of PS back to the PM. These data collectively suggest the involvement of ORP6 in the counter-transport of PI4P and PS.

1. Introduction

Non-vesicular lipid transport by lipid transfer proteins commonly occurs at membrane contact sites (MCSs) where different organelles come in close contact [1]. In mammalian cells, cholesterol and phospholipids are critical components of cellular membranes, forming distinct compositions on each membranous organelle and contribute to cell signaling [2] and vesicular trafficking [3]. Cholesterol and phospholipids, such as phosphatidylcholine, phosphatidylethanolamine, phosphatidylserine (PS) and phosphatidylinositol (PI) are synthesized mainly in the ER or mitochondria and are transported to other organelles through vesicular or non-vesicular transport [4,5].

Members of the Oxysterol-binding protein (OSBP)-related protein (ORP) family are known to localize at MCSs and are involved in the transport of specific lipids between organelles [1,6]. Constituents of the ORP family have a common structure ; an OSBP-related ligand binding domain (ORD) in the C-terminal region, the pleckstrin homology (PH) domain in the N-terminal region and the two phenylalanines in an acidic tract (FFAT) motif between these two domains [1]. These domains function in cargo lipid interaction, non-ER membrane targeting, and ER membrane localization via vesicle-associated membrane protein-associated protein (VAP), respectively [7]. The ORP family consists of 12 proteins and is divided into six subfamilies [8]. OSBP is the first molecule to be identified in the ORP family. It forms a homodimer and localizes to the ER-Golgi MCS where it has a role in the counter-transport of PI4P and cholesterol from the Golgi apparatus to the ER and from the ER to the Golgi apparatus, respectively [1,9,10].

ORP6 is a member of subfamily III along with ORP3 and ORP7. *Orp6* mRNA is abundant in brain and skeletal muscle [11]. ORP6 has also been reported to be involved in the transport of cholesterol between the ER and endosomes in macrophages [12]. ORP6 has been identified in genome-wide, family-based association analysis of Alzheimer's disease [13] and is implicated in autism [14]. We have previously reported that endogenous ORP6 is associated with the ER in neurons and exogenous ORP6 localized to the ER, and ER-plasma membrane (PM) contact sites in cultured cerebellar cells [15]. Overexpression of the ORP6 intermediate region between the PH and ORD domains (ORP6 int) blocks the localization of ORP6 at the PM and partially shifted localization of OSBP PH domain, a PI4P marker to the PM, suggesting the involvement of ORP6 in the turnover of PI4P at ER-PM contact sites. Further investigation of the intracellular function of ORP6 in neuronal lipid transport is

* Corresponding author. 3311-1 Yakushiji, Shimotsuke-shi, Tochigi, 329-0498, Japan.
E-mail address: ynoda@jichi.ac.jp (Y. Noda).

https://doi.org/10.1016/j.bbrep.2022.101257
Received 7 February 2022; Received in revised form 27 March 2022; Accepted 31 March 2022

Abbreviations

DIV	days in vitro
ER	endoplasmic reticulum
FFAT	two phenylalanines in an acidic tract
GalT	1,4-galactosyltransferase
Lact	Lactadherin
MCS	membrane contact site
ORD	OSBP-related ligand binding domain
ORP	oxysterol binding protein-related protein
OSBP	oxysterol-binding protein
PH	pleckstrin homology
PI4KIIIα	phophtidylinositol 4-kinase type IIIα
PI4P	phophtidylinositol-4-phosphate
PM	plasma membrane
PS	phosphatidylserine
PSS1	PS synthase 1
RAB4A	Ras Related Protein 4a
SNAP25	synaptosome associated protein 25
VAP	vesicle-associated membrane protein-associated protein

imperative for elucidation of involvement in neuro-pathogenesis.

In the present study, we searched for lipids transported in exchange for PI4P by ORP6. Knockdown of ORP6 with specific RNAi or over-expression of dominant negative constructs of ORP6 lacking the lipid-binding ORD domain caused the accumulation of a PS marker in the cytoplasm. Blocking synthesis of PI4P at the PM by a PI4KIIIα inhibitor changed the distribution of ORP6 as well as PS. Furthermore, inhibition of PS synthesis at the ER affected the distribution of PI4P at the PM and reduced PS presence at the PM. Introduction of ORP6 but not the dominant negative ORP6 int, alleviated the influence of PS synthesis inhibition and returned PS localization back to the PM. Our data collectively suggest the involvement of ORP6 in the counter-transport of PI4P and PS at ER-PM contact sites.

2. Materials and methods

2.1. cDNA constructs

Full length ORP6 and constructs were obtained as previously described [15]. Briefly, the full-length ORF of mouse Orp6 cDNA (NM_001290733.1) was obtained by PCR by using mouse brain cDNA as a template. The full-length ORF, the PH domain flanked by four amino acids (amino acids 83–187), intermediate region (amino acids 184–594; ORP6 int), truncated form lacking the ORD (ORP6 ΔORD) were cloned into the pEGFP-C1 (Clontech, Mountain View, CA) and pTagRFP-C (Evrogen, Moscow, Russia) vectors, positioning the inserted protein C-terminally and attaching fluorescent proteins or tags to the N-terminal [15]. The single or two tandem PH domains of Osbp (M86917, amino acids 87–189) and the C2 domain of Lactadherin (Lact C2 domain, AK171143) were cloned into the pTagRFP-C vector. Full-length mouse Pss1 (NM_008959.3) and mutant Pss1 enzyme (L265P) were cloned into pEGFP-C1 and Halo Tag (Promega, Madison, WI) vectors. Halo Tag fusion proteins were labeled using Coumarin Ligand. The dye was added to the media and rinsed once. Cell-right ER-RFP marker cDNA and LysoTracker Deep Red were purchased from Molecular probes (Eugene, OR). Cell-right ER-RFP is an expression vector encoding a fusion protein comprised of RFP with the calreticulin ER insertion sequence and the KDEL tetrapeptide retention sequence. Markers for the trans-Golgi membrane, early endosome, and PM were constructed using beta 1, 4-galactosyltransferase (GalT, NM_022305), Rab4a (NM_009003), Snap25 (NM_001291056), respectively. GalT was cloned into pEGFP-N1. Rab4a and Snap25 were cloned into pEGFP-C1 [15].

2.2. Cell culture

Neuro-2A cells were cultured in DMEM (Sigma-Aldrich, St. Louis, MO) supplemented with 10% fetal bovine serum (FBS, Thermo Fisher Scientific) at 37 °C under 5% CO_2. Cerebellar granule cells were extracted from 7-day-old ICR mice (Japan SLC, Inc., Shizuoka, Japan) in accordance with the Animal Care and Use Committee of Jichi Medical University and the ARRIVE guidelines, as described previously [15]. Briefly, mice were anesthetized with vaporized 30% isoflurane and then decapitated, and the cerebella were excised and treated with trypsin-EDTA (Thermo Fisher Scientific, Bothell, WA) for 7 min at room temperature. Dissociated cells were rinsed with HBSS (Wako Pure Chemical Industries, Osaka, Japan) three times and then plated into 4-compartment glass-bottom culture dishes (Greiner Bio-one, Kremsmünster, Austria) at a concentration of 4×10^4/ml cells per well. Cells were kept in 0.5 ml Neurobasal Medium (Thermo Fisher Scientific) supplemented with B27 supplement (Thermo Fisher Scientific).

2.3. Transfection and image acquisition, analysis

Neuro-2A cells and cerebellar granule cells at DIV 4 were transfected using Lipofectamine LTX Plus Reagent (Thermo Fisher Scientific) according to the manufacturer's directions. The cells were imaged by using DeltaVision Elite Microscopy System (GE Healthcare, Brier, WA). A predesigned Stealth RNAi (MSS235331, Thermo Fisher Scientific) was used to knockdown ORP6. FITC labeled oligos or unconjugated RNA were used as negative control (Block-it Fluorescent Oligo or Stealth RNAi siRNAi Negative Control, Thermo Fisher Scientific). RNAi targeting ORP6 decreased the expression of ORP6 to $12.0 \pm 4.8\%$ and $9.9 \pm 8.8\%$, 24 and 48 h after transfection, respectively, compared to control oligos [15]. RNAi transfected cells were imaged 24 h after transfection.

2.4. Filipin staining

Cholesterol in cultured cells was analyzed by filipin (Sigma-Aldrich) staining in accordance with a previous report [16]. Cells were washed with phosphate-buffered saline (PBS, Sigma-Aldrich) three times and were fixed with 4% paraformaldehyde (PFA, Merck, Burlington, MA) in PBS for 1 h at room temperature. Cells were washed with PBS three times and then residual PFA was quenched with 1.5 mg/ml Glycine (Wako Pure Chemical Industries) in PBS for 10 min at room temperature. Cells were incubated with 50 μg/ml filipin in PBS containing 10% FBS for 2 h at room temperature and were washed with PBS three times.

2.5. Treatment with PI4KIIIα inhibitor

Neuro-2A cells in Leibovitz's 15 medium (Thermo Fisher Scientific) were treated with 100 nM PI4KIIIα inhibitor (SML2453, Sigma-Aldrich) in dimethyl sulfoxide (DMSO, final concentration 0.1%). The cells were imaged before and after treatment with PI4KIIIα inhibitor by using the DeltaVision Elite Microscopy System. The total amount of PI4P and PS on the PM of cells was observed by acquiring images at 0.5 μm intervals in the z-axis direction for a total of 5 μm to ascertain reduction at the PM of the whole cell.

2.6. Statistical analysis

For knockdown experiments, cultured cerebellar neurons were transfected with the Lact C2 domain together with either control RNA or RNAi targeting ORP6 (control; $n = 105$, RNAi; $n = 107$) and were categorized into three groups based on the signal intensity of Lact C2 domain at the PM and accumulation in the cytoplasm; cells with PM maximum fluorescence intensity of more than four hundred arbitrary units (a. u.) (PM $>$ 400 a. u.), cells with PM maximum fluorescence of less than four hundred a. u. containing only small puncta in the cytoplasm (PM $<$ 400 a. u.) and cells with PM maximum fluorescence of less

than four hundred a. u. containing puncta with a diameter greater than 1 μm (PM < 400 a. u. with accumulation). Data were collected from seven independent experiments and the percentage of each three groups are shown as the mean ± SE, respectively. The results were statistically analyzed using Welch's *t*-test. A P value of less than 0.05 was considered statistically significant [15]. For dominant negative experiments, cultured cerebellar neurons were transfected with Lact C2 domain and full length ORP6 (n = 104), ORP6 int (n = 103) or ORP6 ΔORD (n = 104) and were categorized into three groups based on the maximum signal intensity of the Lact C2 domain at the PM as described above.

To examine cholesterol localization, cultured cerebellar neurons were transfected with either control RNA or RNAi targeting ORP6 (control; n = 104, RNAi; n = 104), then stained with filipin and categorized into two groups based on the maximum signal intensity of filipin at the PM with a threshold of eight hundred a. u. Data were collected from five independent experiments. Percentage of each two groups are shown as the mean ± SE, respectively. The results were statistically analyzed using Welch's *t*-test. A P value less than 0.05 was considered statistically significant.

To analyze the colocalization of PS with organelle markers when ORP6 was knocked down, Pearson's correlation coefficient was calculated between GFP-Lact C2 and ER-RFP (control; n = 29, RNAi; n = 30) or LysoTracker Deep Red (control; n = 30, RNAi; n = 31) GFP-RAB4A and RFP-Lact C2 (control; n = 30, RNAi; n = 30) or GalT-GFP and RFP-Lact C2 (control; n = 30, RNAi; n = 29) in cells transfected with either control RNA or RNAi targeting ORP6. Data were collected from three independent experiments and the values for each group are shown as mean ± SE. Statistical analysis was performed using Welch's *t*-test. A P value less than 0.05 was considered statistically significant.

To analyze the colocalization of ORP6 deleted constructs with organelle markers, Pearson's correlation coefficient was calculated between GFP-ORP6 int and ER-RFP (n = 32) or RFP-SNAP25 (n = 37), or between GFP-ORP6 ΔORD and ER-RFP (n = 33) or RFP-SNAP25 (n = 32). Data were collected from three independent experiments and the values for each group are shown as mean ± SE. Statistical analysis was performed using Welch's *t*-test. A P value less than 0.05 was considered statistically significant.

Pearson's correlation coefficient was also calculated for the co-localization of GFP-SNAP25 and RFP-OSBP2 × PH before and after treatment with DMSO (n = 30) or PI4KIIIα inhibitor (n = 30). Data were collected from four independent experiments.

Co-localization between GFP-SNAP25 and RFP-ORP6 or GFP-SNAP25 and RFP-Lact C2 before and after treatment with DMSO (n = 30, 31, respectively) or PI4KIIIα inhibitor (n = 31,30, respectively) was evaluated using Pearson's correlation coefficient, respectively. Data were collected from six independent experiments.

Neuro-2A cells expressing the PH domain of ORP6 were treated with DMSO (n = 102) or PI4KIIIα inhibitor (n = 105) and were categorized into two groups based on the maximum signal intensity of ORP6 PH domain at the PM with a threshold of eight hundred a. u. Data were collected from five independent experiments. The percentage of each of the two groups are shown as the mean ± SE, respectively. The results were statistically analyzed using Welch's *t*-test. A P value less than 0.05 was considered statistically significant.

Pearson's correlation coefficient was calculated for the co-localization with RFP-Lact C2 and GFP (n = 34), GFP-PSS1 (n = 35) or GFP-PSS1L265P (n = 36). Data were collected from three independent experiments and the values for each group are shown as mean ± SE.

Pearson's correlation coefficient was calculated for the co-localization with GFP-SNAP25 and RFP-OSBP PH together with Halo tag (n = 32), Halo-PSS1 (n = 30) or Halo-PSS1L265P (n = 31). Data were collected from three independent experiments and the values for each group are shown as mean ± SE.

Pearson's correlation coefficient was calculated for the co-localization between RFP-Lact C2, Halo-PSS1L265P and either GFP (n = 40), GFP-ORP6 (n = 47), GFP-ORP6 int (n = 45) or GFP-ORP6 ΔORD (n = 43). Data were collected from three independent experiments and the values for each group are shown as mean ± SE. All the results were statistically analyzed using Kruskal-Wallis test and Steel's multiple comparison test. A P value less than 0.05 was considered statistically significant.

3. Results

3.1. ORP6 RNAi changed the localization of the PS marker

Our previous report has shown that ORP6 is involved in the transport of PI4P in primary cultured cerebellar neurons. To look for the lipid that is counter-transported, we examined the distribution of two candidates, free cholesterol and PS in neurons subjected to ORP6 knockdown by using RNAi. Filipin, specifically binding to free cholesterol, distributed to the PM and cytoplasm [16,17] and did not change localization (Fig. 1D–F) while the fluorescently tagged C2 domain of Lactadherin (Lact C2 domain), which binds specifically to PS [18–20], diminished in most cells at the PM compared to control RNAi transfected cells (Fig. 1A–C). The percentage of cells with the maximum PM fluorescence intensity of more than four hundred arbitrary units (a. u.) (PM > 400 a. u.) significantly decreased from 54.8% ± 6.2–21.3% ± 4.9 when under the influence of ORP6 RNAi (Fig. 1C). While reduced at the PM, more Lact C2 domain accumulated from 6.3% ± 2.2–44.4% ± 6.2 in the cytoplasm.

Pearson's correlation coefficient between the two fluorescent markers revealed that cytoplasmic Lact C2 domain signals partially colocalized with ER marker (Fig. 2A–C, statistics in M, ORP6 RNAi versus control RNA: r = 0.61 ± 0.03 versus 0.51 ± 0.03), and the lysosome marker, LysoTracker Deep Red (arrows, Fig. 2D–F, statistics in M, ORP6 RNAi versus control RNA: r = 0.66 ± 0.02 versus 0.48 ± 0.02) and also with the early endosome marker, RAB4A (Fig. 2D–F, ORP6 RNAi versus control RNA: 0.59 ± 0.03 versus 0.6 ± 0.03), but not with a Golgi marker, GalT (Fig. 2G–I, ORP6 RNAi versus control RNA: 0.36 ± 0.03 versus 0.31 ± 0.04). The distribution of Lact C2 domain in cells transfected with respective organelle markers and control RNA is shown in Fig. S1. PS is known to be synthesized at the ER then transported to other parts of the cell, especially to the PM [4,21], thus the decrease in localization of PS at the PM suggests that the knockdown of ORP6 prevented PS transport to the PM from the ER.

3.2. The intermediate region and other deletion mutants lacking the ORD of ORP6 changed localization of the PS marker

Next, we constructed dominant negative forms of ORP6 which lack functional domains (Fig. 3A) and evaluated their inhibitory effects. Fig. 3 shows Neuro-2A cells transfected with two constructs, one with the ORD and PH domain deleted (ORP6 int, Fig. 3B–G) and one lacking only the ORD (ORP6 ΔORD, Fig. 3H-M). Both constructs lack ORD, a lipid binding domain located at the C-terminal and is the defining domain of OSBP-related proteins. Reflecting presence of the PH domain that functions to target ORP6 to the PM, the latter construct localized at the PM (r = 0.66 ± 0.03) but the former (r = 0.4 ± 0.03) did not (Fig. 3E–G, K-M, statistics shown in N).

In cerebellar neurons expressing ORP6 int (Fig. 4D–F) or ORP6 ΔORD (Fig. 4G–I), Lact C2 domain localized at the PM significantly decreased and accumulated in the cytoplasm (Fig. 4D–I, statistics shown in J) compared to cells expressing ORP6 (Fig. 4A–C). These results are identical to the effect of ORP6 RNAi. Overexpression of both constructs affected the localization of PS, suggesting the ORD domain functions to transport PS.

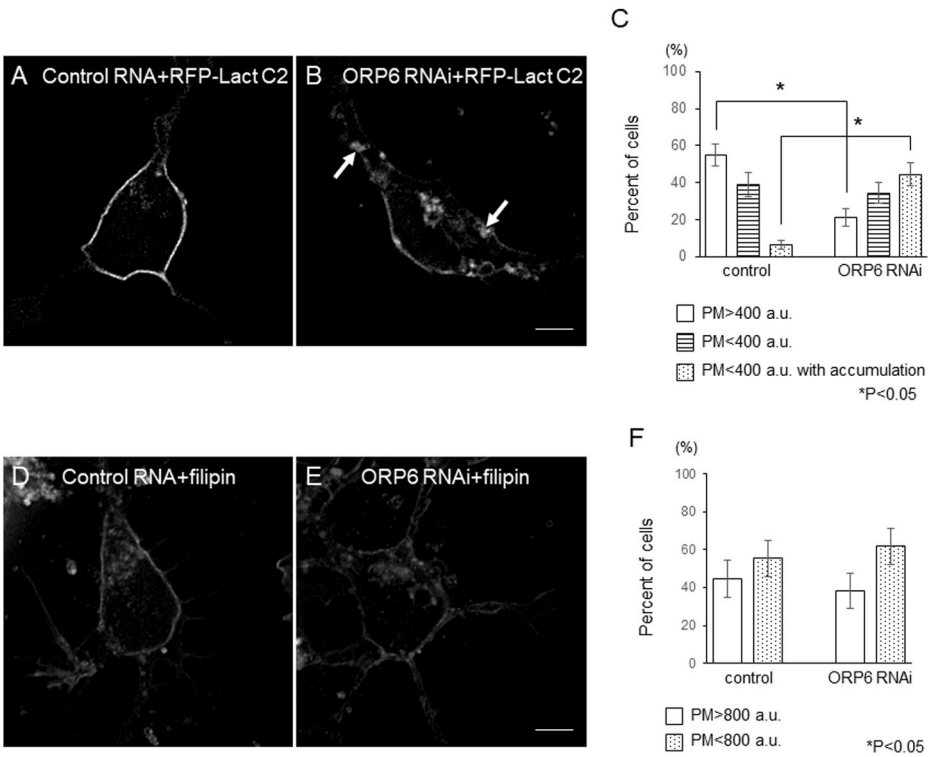

Fig. 1. ORP6 RNAi partially shifted a PS marker from the PM to the cytoplasm in cerebellar neurons. Localization of RFP-Lact C2, a PS marker, in control RNA transfected cells (A), and ORP6 RNAi transfected cells (B). Arrows indicate accumulation of RFP-Lact C2 domain in cytoplasm. Bars, 10 μm. (C) Percentage of cells sorted by localization of Lact C2 domain; cells with a maximum PM fluorescence intensity of more than four hundred arbitrary units (a. u.) (PM > 400 a. u.), cells with a maximum PM fluorescence of less than four hundred a. u. (PM < 400 a. u.), and cells with a maximum PM fluorescence less than four hundred a. u. containing puncta with a diameter greater than 1 μm (PM < 400 a. u. with accumulation). Data were collected from seven independent experiments (control; n = 105, RNAi; n = 107) and the percentage of each three groups are shown as the mean ± SE. We used Welch's *t*-test to evaluate statistical significance (*P < 0.05). Images of cerebellar cells transfected with control RNA (D) or RNAi targeting ORP6 (E) stained with filipin. (F). Percentage of cells that have a maximum fluorescence intensity of filipin at PM of more than eight hundred a. u., (PM > 800 a. u.), or less than eight hundred a. u. (PM < 800 a. u.). Data were collected from five independent experiments (control; n = 104, RNAi; n = 104) and the percentage of two groups are shown as the mean ± SE, respectively. Bar indicates 10 μm.

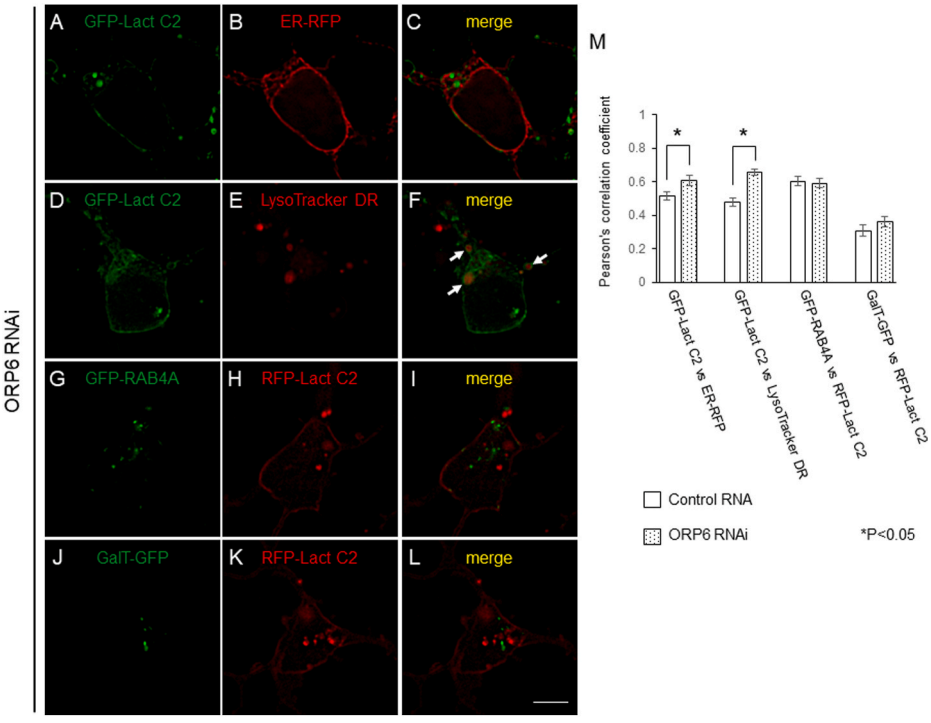

Fig. 2. ORP6 RNAi caused PS accumulation at lysosomes and ER but did not affect Golgi or early endosomes in cerebellar neurons. Cerebellar granule cells were co-transfected with ORP6 RNAi and the following constructs or staining; GFP-Lact C2 and ER-RFP (A–C), GFP-Lact C2 and stained with LysoTracker Deep Red (lysosome) (D–F), GFP-RAB4A (early endosome) and RFP-Lact C2 (G–I), GalT-GFP (Golgi) and RFP-Lact C2 (J–L). Arrows indicate co-localization of GFP-Lact C2 and LysoTracker Deep Red. (M) Pearson's correlation coefficient was calculated for co-localization between GFP-Lact C2 and ER-RFP (control; n = 29, RNAi; n = 30), or LysoTracker Deep Red (control; n = 30, RNAi; n = 31), RFP-Lact C2 and GFP-RAB4A (control; n = 30, RNAi; n = 30) or GalT-GFP (control; n = 30, RNAi; n = 29) in cells treated with either control RNA or ORP6 RNAi. Data were collected from three independent experiments. Bars, 10 μm. Corresponding control RNA experiments are shown in Fig. S1. (For interpretation of the references to colour in this figure legend, the reader is referred to the Web version of this article.)

3.3. Treatment with a PI4KIIIα inhibitor suppressed the localization of the PI4P marker as well as ORP6 and the PS marker, at the PM

We have previously reported that the overexpression of ORP6 int induced retention of PI4P at the PM [15]. Since the counter transport of lipids at MCSs is driven by the active gradient of PI4P by phosphorylation-dephosphorylation reactions [22], we treated Neuro-2A cells with an inhibitor of PI4KIIIα, which synthesizes PI4P at the PM by phosphorylating PI [23–25]. We first examined the effect of the PI4KIIIα inhibitor on the distribution of PI4P at the PM, by using fluorescently tagged two-tandem OSBP PH domains (OSBP2 × PH) as a PI4P marker. OSBP2 × PH predominantly localized to the PM with SNAP25 (Fig. 5A–F) as previously reported [26]. Treatment with the PI4KIIIα inhibitor decreased the localization of OSBP2 × PH at the PM after 60 min and 12 h (Fig. 5G-L, M), reflecting inhibition of PI4P synthesis. Pearson's correlation coefficient, quantifying co-localization

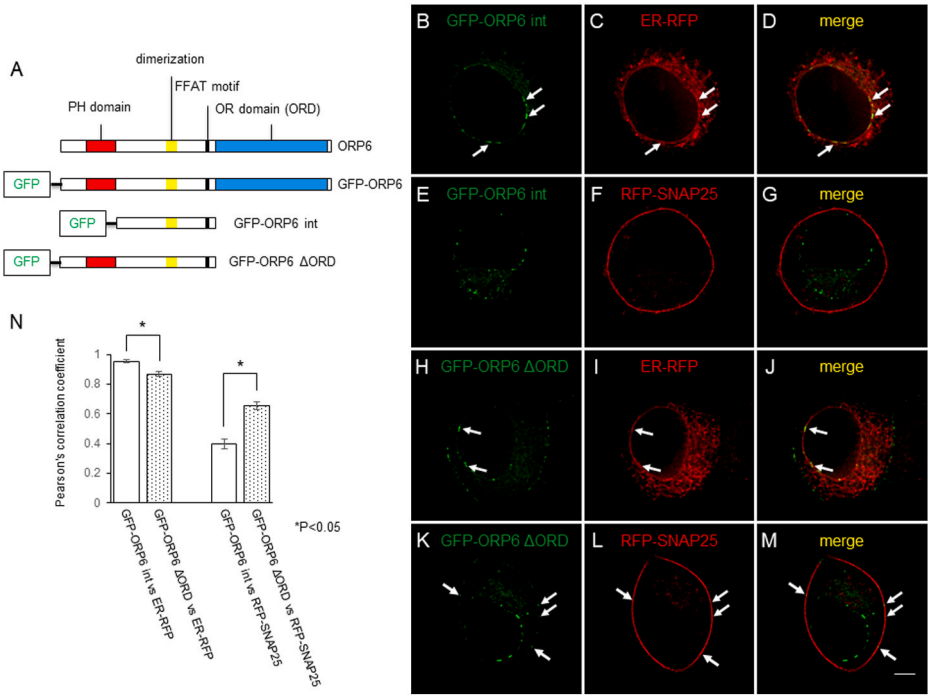

Fig. 3. Localization of ORP6 deletion mutants in Neuro-2A cells. (A) Domain structure of constructs of ORP6. (B–D) Images of Neuro-2A cells co-transfected with GFP-ORP6 int and ER-RFP (ER). Arrows indicate co-localization. (E–G) Cells co-transfected with GFP-ORP6 int and RFP-SNAP25 (PM). (H–J) Images of Neuro-2A cells co-transfected with GFP-ORP6 ΔORD and ER-RFP. Arrows indicate co-localization. (K–M) Cells co-transfected with GFP-ORP6 ΔORD and RFP-SNAP25. Arrows indicate co-localization (N) Pearson's correlation coefficient was calculated for co-localization between GFP-ORP6 int and ER-RFP (n = 32) or RFP-SNAP25 (n = 37) and GFP-ORP6 ΔORD and ER-RFP (n = 33) or RFP-SNAP25 (n = 32). Data were collected from three independent experiments and the values for each group are shown as mean ± SE. Statistical analysis was performed using Welch's *t*-test. A P value less than 0.05 was considered statistically significant. Bars, 10 μm.

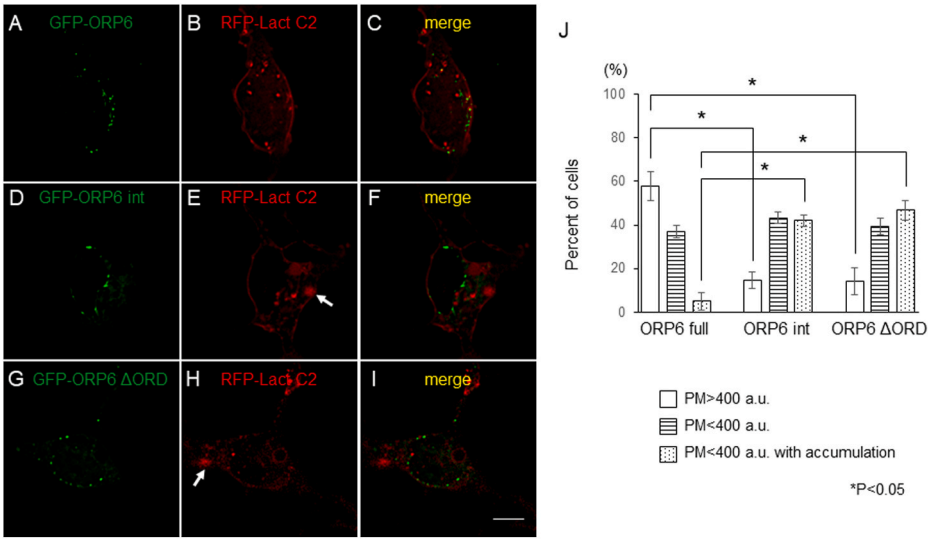

Fig. 4. ORP6 int and ORP6 ΔORD partially shifted PS marker from PM to cytoplasm in cerebellar neurons. Cerebellar granule cells were transfected with RFP-Lact C2 and either GFP-ORP6 (A–C), GFP-ORP6 int (D–F) or GFP-ORP6 ΔORD (G–I). (J) Percentage of cells with maximum Lact C2 fluorescence at the PM of more than four hundred a. u. (PM > 400 a. u.) or less than four hundred a. u., (PM < 400 a. u.), or less than four hundred a. u. and containing puncta with a diameter greater than 1 μm (PM < 400 a. u. with accumulation). Data were collected from six independent experiments (ORP6; n = 104, ORP6 int; n = 103 and ORP6 ΔORD; n = 104) Bars, 10 μm.

between GFP-SNAP25 and RFP-OSBP2 × PH, significantly decreased after 60 min (r = 0.79 ± 0.03 versus r = 0.93 ± 0.01) and 12 h (r = 0.75 ± 0.02 versus r = 0.92 ± 0.01) compared to control cells treated with DMSO (Fig. 5D–F, J-L, M).

We also observed the localization of ORP6 in Neuro-2A cells. ORP6 shifted predominantly to the cytoplasm and localization at the PM significantly decreased 60 min and 12 h after treatment (Fig. 6G-L, M) compared to control (Fig. 6A–F, M); r = 0.52 ± 0.02 versus r = 0.65 ± 0.02 and 0.52 ± 0.03 versus 0.66 ± 0.02, at 60 min and 12 h, respectively. The PH domain of ORP6, which we previously reported binds PI4P at the PM, also decreased at the PM and appeared diffusely throughout the cytoplasm after treatment with the PI4KIIIα inhibitor. The population of cells expressing the PH domain of ORP6 with a maximum fluorescence intensity of more than eight hundred a. u. at the PM significantly decreased 60 min after treatment with the PI4KIIIα inhibitor (Figs. S2C, D, E), compared to control treated with DMSO (Figs. S2A, B, E): 41.2% ± 6.7 versus 82.6% ± 4.9, which reflects the PI4P dependent localization of ORP6 at the PM.

We further analyzed the dynamics of PS in Neuro-2A cells treated with the PI4KIIIα inhibitor. Localization of Lact C2 domains at the PM was suppressed 12 h after treatment with PI4KIIIα inhibitor. Pearson's correlation coefficient index showed that localization of Lact C2 domain at the PM significantly decreased 12 h after treatment (Fig. 7G-L, M) compared to control (Fig. 7A–F, M); r = 0.68 ± 0.03 versus r = 0.9 ± 0.02, similar to as reported by Sohn [23].

Deceased PM PI4P affected localization of ORP6 and transport of PS to the PM: Together with results of reduced PM localization of PS by ORP6 RNAi and ORP6 dominant negative constructs, these data collectively implicate ORP6 in the transport of PS to the PM.

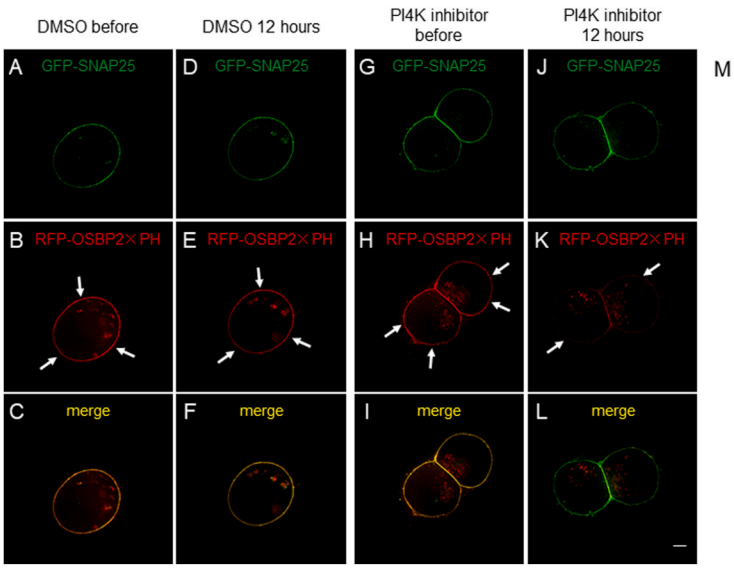

Fig. 5. PI4KIIIα inhibitor treatment decreased PI4P marker at PM decreased in Neuro-2A cells. Cells were co-transfected with GFP-SNAP25 (PM) and RFP-OSBP2 × PH, a PI4P marker. Before (A–C) or 12 h after treatment with DMSO (D–F). Before (G–I) or 12 h after treatment with PI4KIIIα inhibitor (J–L). Arrows indicate PM localized RFP-OSBP2 × PH. (M) Pearson's correlation coefficient was calculated for the co-localization of GFP-SNAP25 and RFP-OSBP2 × PH before and after treatment with DMSO (n = 30) or PI4KIIIα inhibitor (n = 30). Data were collected from four independent experiments and the values for each group are shown as mean ± SE. Statistical analysis was performed using Welch's *t*-test. A P value less than 0.05 was considered statistically significant. Bars, 10 μm.

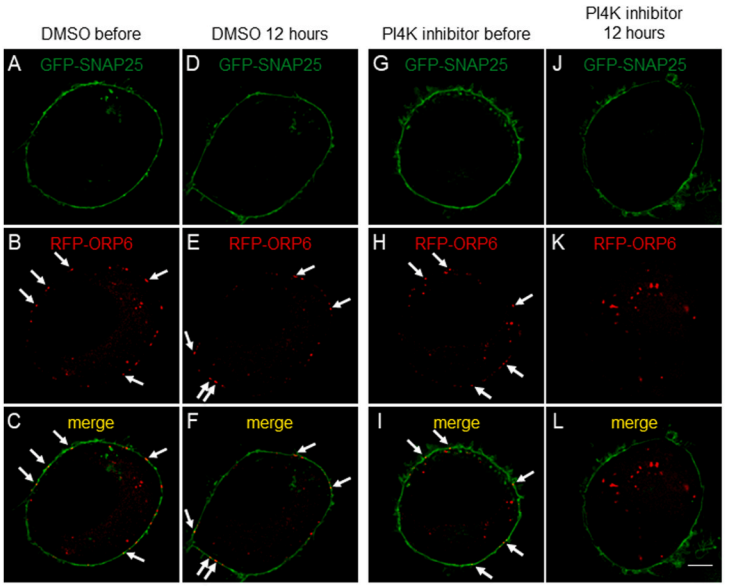

Fig. 6. PI4KIIIα inhibitor treatment dislodged ORP6 from the PM in Neuro-2A cells. Cells were co-transfected with GFP-SNAP25 (PM) and RFP-ORP6. Before (A–C) or 12 h after treatment with DMSO (D–F). Before (G–I) or 12 h after treatment with PI4KIIIα inhibitor (J–L). Arrows indicate co-localization of GFP-SNAP25 and RFP-ORP6. (M) The co-localization between GFP-SNAP25 and RFP-ORP6 before and after treatment with DMSO (n = 30) or PI4KIIIα inhibitor (n = 31) was evaluated using Pearson's correlation coefficient. Data were collected from six independent experiments and the values for each group are shown as mean ± SE. Bars, 10 μm.

3.4. Mutant PSS1 enzyme changed the localization of the PI4P marker

PS is synthesized from phosphatidylcholine or phosphatidylethanolamine in the ER by PS synthase 1/2 (PSS1/2) and is transported mainly to the PM [21,27,28]. Transfection of mutant PSS1 enzyme (PSS1L265P), insensitive to feedback inhibition, produces excessive PS in the ER [23]. We first examined the localization of the PS marker in Neuro-2A cells transfected with PSS1L265P. In cells expressing wild type PSS1 enzyme (Fig. 8D–F), Lact C2 domain mainly localized to the PM and cytoplasm. Cytoplasmic Lact C2 domain colocalized with PSS1 at the ER after 24 h. But in cells expressing PSS1L265P, localization of Lact C2 domain at the PM decreased and increased in the cytoplasm (Fig. 8G–I statistics shown in J). Pearson's correlation coefficient showed that localization of Lact C2 domain at the ER significantly increased in cells expressing PSS1L265P compared to wild type PSS1; r = 0.85 ± 0.02 versus 0.63 ± 0.02, respectively.

To examine whether PI4P is counter-transported in exchange for PS, we observed the localization of fluorescently tagged PI4P marker in cells expressing PSS1L265P. We used fluorescently tagged single OSBP PH domain. We previously reported that this domain mainly localized to the Golgi apparatus but partially shifted to the PM in the presence of ORP6 int [15]. Along with RFP-OSBP PH and GFP-SNAP25, we conducted triple transfections using either Halo Tag or Halo-PSS1 or Halo-PSS1L265P. In cells expressing Halo Tag (Fig. 9A–D) or wild type PSS1 enzyme (Fig. 9E–H), the single OSBP PH domain mainly localized to the Golgi apparatus. Pearson's correlation coefficient showed that localization of single OSBP PH domain at the PM increased in cells expressing PSS1L265P (Fig. 9I-L) compared to Halo Tag only (Fig. 9A–D) or wild type PSS1 (Fig. 9E–H). The increase of PM PI4P is statistically significant (Fig. 9M: r = 0.66 ± 0.03 versus 0.34 ± 0.03 versus 0.38 ± 0.04, respectively), implying retention of PS at the ER leading to a shift in PI4P at the PM similar to the results from ORP6 RNAi and dominant negative experiments shown above.

Lastly, we overexpressed GFP, ORP6, ORP6 int or ORP6 ΔORD in cells along with mutant PSS1 and Lact C2 domain. In cells expressing GFP only, Lact C2 domain localized to cytoplasm and PM (Fig. 10A–D), the same as Fig. 8H. Lact C2 colocalized well with mutant PSS1 (Fig. 10Q, r = 0.84 ± 0.02). In cells expressing ORP6 int or ORP6 ΔORD,

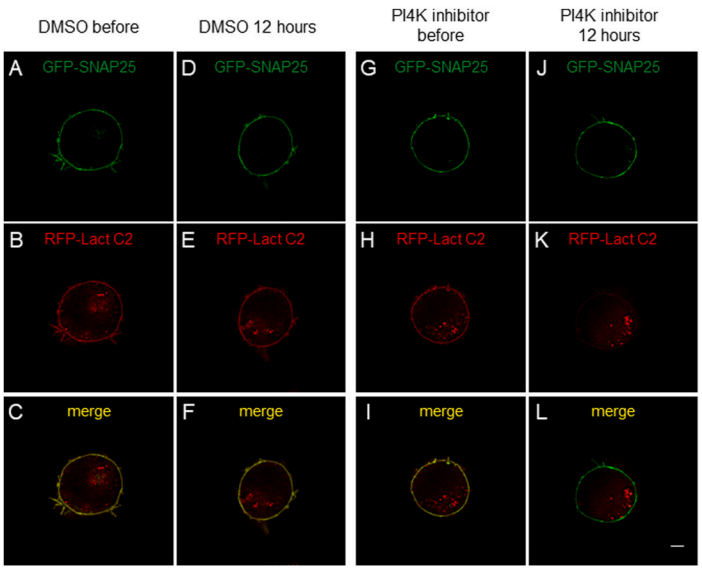

Fig. 7. Localization of PS marker at PM was suppressed by PI4KIIIα inhibitor treatment in Neuro-2A cells. Co-transfection of GFP-SNAP25 and RFP-Lact C2, a PS marker, before (A–C) or 12 h after treatment with DMSO (D–F), before (G–I) or 12 h after treatment with PI4KIIIα inhibitor (J–L). (M) Pearson's correlation coefficient was calculated for the co-localization of GFP-SNAP25 and RFP-Lact C2 before and after treatment with DMSO (n = 31) or PI4KIIIα inhibitor (n = 30). Data were collected from four independent experiments and the results for each group are shown as mean ± SE. Statistical analysis was performed using Welch's *t*-test. A P value less than 0.05 was considered statistically significant.

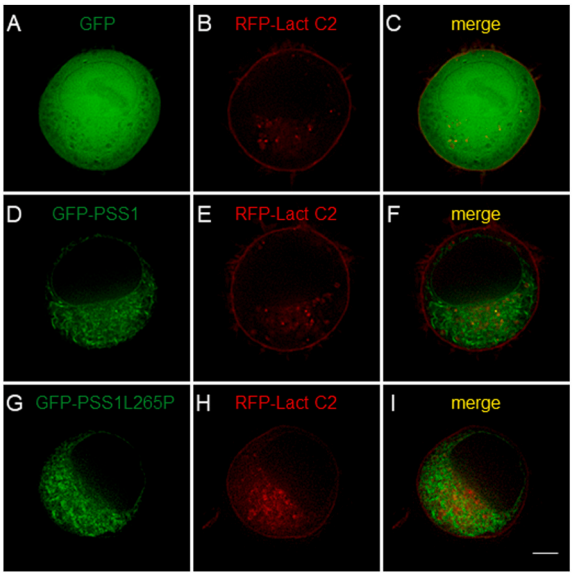

Fig. 8. Overexpression of mutant PSS1 altered the localization of PS marker in Neuro-2A cells. Co-transfection of RFP-Lact C2, a PS marker with either GFP (A–C), GFP-phosphatidylserine synthase 1 (PSS1, D-F) or GFP- PSS1L265P (G–I). (J) Pearson's correlation coefficient was calculated for the co-localization with RFP-Lact C2 and GFP, GFP-PSS1 or GFP-PSS1L265P. Data were collected from three independent experiments (GFP n = 34, GFP-PSS1 n = 35 and GFP-PSS1L265P n = 36). Bars, 10 μm.

Lact C2 domain remained cytoplasmic, co-localizing well with mutant PSS1 (Fig. 10I-P, Q, r = 0.85 ± 0.02 or 0.87 ± 0.01, respectively). In contrast, ORP6 increased PS at the PM and significantly decreased cytoplasmic PS (Fig. 10E–H, Q, r = 0.78 ± 0.02), suggesting that ORP6 contributed in the transfer of overproduced PS from the ER to PM in cells expressing mutant PSS1 and that the ORD of ORP6 is involved in this process.

Together with our previous work showing that ORP6 colocalized with the ER-PM contact site marker at the PM [15], the present data clearly demonstrate ORP6 localizing to ER-PM contact sites by binding to PM PI4P through the PH domain, recruiting PS from the ER through the ORD in exchange for PI4P thus contributing to the counter-transport of PS and PI4P between the ER and PM in neurons.

4. Discussion

Here, we report that knockdown or dominant negative inhibition of ORP6 suppressed transfer of PI4P and PS between the ER and PM in neurons. Perturbing the localization of either lipid affected the distribution of the other and ORP6. Depletion of PI4P at the PM decreased PS and ORP6 at the PM. We previously reported that ORP6 localizes to ER-PM contact sites and that its PH domain bound to PI4P and is anchored to the PM [15], however our study did not extend to the C-terminal ORD domain which is predicted to bind lipids as demonstrated in other ORPs [1,10]. Indeed, deletion of ORD domain or expression of ORP6 int which lacks the PH and ORD domains affected the transport of PS in a manner identical to the knockdown of ORP6 (Fig. 4). Additionally, ORP6 but not ORP6 int or ORP6 ΔORD could return PS to the PM when PSS1L265P induced overproduction of PS at the ER (Fig. 10), suggesting that the ORD domain is essential for transport of PS. Taken collectively, these data suggest ORP6 has a possible role in the counter-transport of PI4P from the PM to ER and PS from the ER to PM by direct or indirect manner.

Most PH domains of ORPs bind to PI4P [1], and we used two constructs to visualize PI4P on membranes; single or two tandem OSBP PH domains in the present report, which allowed us to visualize PI4P on the Golgi apparatus and PM, respectively. Although this method has been extensively used [24,26], the mechanism of how the tandem OSBP PH domains come to recognize PI4P on the PM rather than Golgi apparatus is unknown. OSBP PH domain recognized PI4P at the PM rather than at

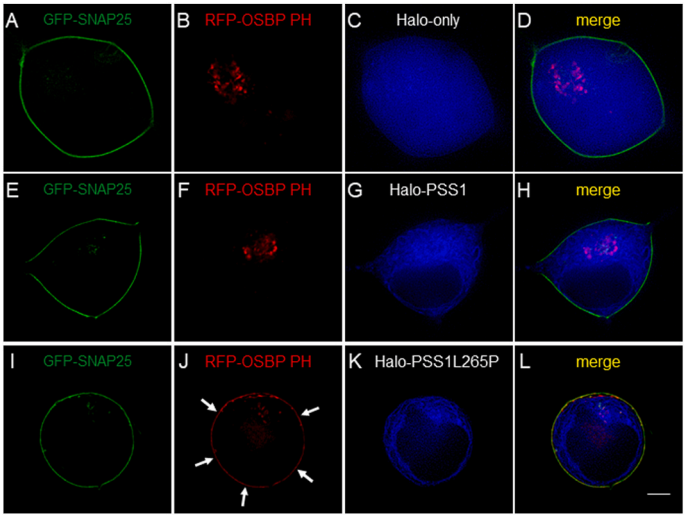

Fig. 9. GFP-PSS1L265P partially shifted the PI4P marker from the Golgi to the PM in Neuro-2A cells. (A–L) Neuro-2A cells triply co-transfected with GFP-SNAP25 (A, E, I), the PH domain of OSBP (OSBP PH, B, F, J) and Halo Tag only (C) or Halo-PSS1 (G) or Halo-PSS1L265P (K). (M) Pearson's correlation coefficient was calculated for the co-localization with GFP-SNAP25 and RFP-OSBP PH together with Halo tag or Halo-PSS1 or Halo-PSS1L265P, respectively. Data were collected from three independent experiments and the values for each group are shown as mean ± SE. The results were statistically analyzed using Kruskal-Wallis test and Steel's multiple comparison test. A P value less than 0.05 was considered statistically significant. Arrows indicate PI4P marker partially shifted from the Golgi to PM. Bars, 10 μm.

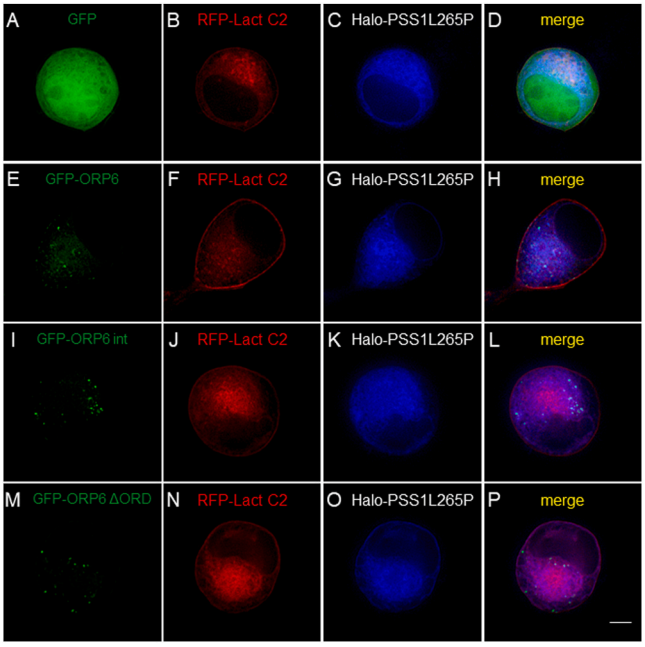

Fig. 10. Overexpression of ORP6 but not ORP6 int or ORP6 ΔORD increased PS marker at the PM in cells expressing mutant PSS1. (A–P) Neuro-2A cells were triply co-transfected with RFP-Lact C2, Halo-PSS1L265P and either GFP only (A–D) or GFP-ORP6 (E–H) or GFP-ORP6 int (I–L) or GFP-ORP6 ΔORD (M–P). (Q) Pearson's correlation coefficient was calculated for the co-localization with RFP-Lact C2 and Halo- PSS1L265P together with GFP or GFP-ORP6 or GFP-ORP6 int or GFP-ORP6 ΔORD. Data were collected from three independent experiments and the values for each group are shown as mean ± SE. The results were statistically analyzed using Kruskal-Wallis test and Steel's multiple comparison test. A P value less than 0.05 was considered statistically significant. Bars, 10 μm.

the Golgi apparatus, which increased in Neuro-2A cells transfected with ORP6 int or with PSS1L265P. In contrast, Sohn et al. [23] reported a decrease of PI4P at the PM which was identified using an antibody in HEK-293 cells transfected with PSS1S269S. This discrepancy may be attributed to the difference in the method of PI4P detection, difference in the cells used or the different PSS1 mutant. Although OSBP PH is known to recognize PI4P [1], there may be other phosphatidylinositides that it binds. ORP6 did not localize to the PM in cells treated with PI4KIIIα inhibitor (Figs. 6K and 7K, Fig. S2), indicating ORP6 PH domain binds to PI4P and ORP6 PM localization is dependent on PI4P as we have previously reported [15]. RFP-OSBP2 × PH also drastically reduced PM localization after PI4KIIIα inhibitor treatment (Fig. 5K) as previously reported [26] suggesting it does indeed recognize PI4P and some ORP6 was found at the PM even with PSS1L265P expression (Fig. 10M – P).

The intermediate region of ORP6, the part encoded by our ORP6 int construct, contains a region functioning in dimerization in addition to the FFAT motif which binds to the ER via VAP [15]. Transfection of ORP6 int localized to the ER but not at ER-PM contact sites (Fig. 3B–G). ORP6 int most likely exerts a dominant negative effect by occupying VAP's FFAT binding site on the ER, or through dimerization with endogenous ORP6 or ORP3. Indeed, we have previously shown that ORP6 int co-immunoprecipitated ORP6 and ORP3 [15]. Although we did not refer to the involvement of ORP3 in the present report, it is possible that ORP3 may dimerize with ORP6 and function in this transport system as a heterodimer. However, the phenotype of dominant negative ORP6 is same as that of ORP6 knockdown, suggesting that ORP3 alone is insufficient to compensate for the loss of function of ORP6. Additional experiments will be needed to reveal the interaction between ORP6 and ORP3.

A past study has revealed that knockdown of ORP6 caused the accumulation of endocytosed cholesterol in macrophages [12]. However, we could not detect a change in filipin staining by RNA-mediated knockdown of ORP6 in Neuro-2A cells (Fig. 1D–F). The central nervous system is rich in cholesterol, which must be *de novo* synthesized because the blood brain barrier blocks the passage of plasma lipoproteins [29]. Thus, cholesterol transport may differ between neurons and other cell types, such as macrophages which undergo frequent phagocytosis and incorporate lipoprotein exogenously [30]. Another possibility is that we

may not have detected the minor population of transported cholesterol compared to the large amount that resides in the PM by filipin staining. Another approach will be needed to clarify the function of ORP6 in cholesterol metabolism.

ORP5 and 8, a member of different subfamily of ORPs, is known to be involved in the counter-transport of PI4P and PS at ER-PM contact sites and resides at the ER through a C-terminal transmembrane domain instead of the FFAT motif [21]. In spite of their similar function in neurons, ORP5 did not colocalize with ORP6 nor did it coimmunoprecipitate [15], suggesting the two ORPs function independent of each other. In primary cultured cerebellar neurons, ORP5 is highly expressed on days 2 and 3 in vitro, and decreases after day 5 in vitro (unpublished data), whereas ORP6 is highly expressed in cultured cerebellar neurons after day 5 in vitro, indicating different expression timing during the development of neurons. ORP8 has been reported to suppress expression of a lipid transporter by interacting with a transcription factor thereby indirectly affecting cholesterol efflux [31]. Thus, the effects an ORP has on a lipid need not be via a physical interaction. The question of whether overexpression or downregulation of ORP6 affects the expression or localization of ORP5 and ORP8 is yet to be addressed as all three proteins are reported to function in the transport of PI4P and PS. Further work is expected to reveal the interactions between ORP6 and ORP5 or ORP8 in lipid transport.

Some ORPs are expressed in the nervous system and apparently involved in its development and maintenance [32,33]. Knockdown of OSBP induces neurite elongation in cerebral cortical neurons. ORP3 modifies the phenotype of amyotrophic lateral sclerosis-linked VAPB. ORP6 is implicated in the pathogenesis of Alzheimer's disease and autism. Further investigation of the intracellular dysfunction of subfamily III members, such as ORP6 and ORP3 in neuronal lipid transport, is imperative for the elucidation of the neuro-pathogenesis of these diseases.

5. Conclusions

We have previously reported that ORP6 is involved in the turnover of PI4P at ER-PM contact sites in neurons. In the present study, we have identified that PS is counter-transported in exchange for PI4P by ORP6. Over-expression of the intermediate region or deletion mutant lacking ORD and RNA-mediated knockdown of ORP6 significantly reduced the PS marker Lact C2 and caused its accumulation in the cytoplasm. Reduction of PM PI4P by PI4K inhibitor treatment significantly suppressed the localization of PS marker and ORP6 at the PM implying counter-transport obstruction. ORP6 but not ORP6 int or ORP6 ΔORD restored PS to the PM when expression of mutant PSS1 induced overproduction of PS at the ER. This indicates the ORD was required for PS transport by ORP6 and we have previously shown that PI4P transport by ORP6 requires the PH domain and the ORD. Taken collectively, these data suggest ORP6 regulates PI4P and PS transport, though whether this occurs by direct action or not would require further study.

Declaration of competing interest

The authors have no conflicts of interest directly relevant to the content of this article.

Acknowledgements

We are grateful to Yukiharu Kido for research assistance and Terue Kikuchi for secretarial assistance and to Professor Nobuhiko Ohno at Jichi Medical University and his lab members for critical discussions and technical assistance. This study was supported by the Jichi Medical University Young Investigator Award.

Appendix A. Supplementary data

Supplementary data to this article can be found online at https://doi.org/10.1016/j.bbrep.2022.101257.

References

[1] V.M. Olkkonen, OSBP-related protein family in lipid transport over membrane contact sites, Lipid Insights 8 (2015) 1–9, https://doi.org/10.4137/LPI.S31726.
[2] S. Eaton, Multiple roles for lipids in the Hedgehog signalling pathway, Nat. Rev. Mol. Cell Biol. 9 (2008) 437–445, https://doi.org/10.1038/nrm2414.
[3] G. D'Angelo, M. Vicinanza, A. Di Campli, M.A. De Matteis, The multiple roles of PtdIns(4)P – not just the precursor of PtdIns(4,5)P2, J. Cell Sci. 121 (2008) 1955–1963, https://doi.org/10.1242/jcs.023630.
[4] S.J. Stone, J.E. Vance, Phosphatidylserine synthase-1 and -2 are localized to mitochondria-associated membranes, J. Biol. Chem. 275 (2000) 34534–34540, https://doi.org/10.1074/jbc.m002865200.
[5] J.E. Vance, Phospholipid synthesis and transport in mammalian cells, Traffic 16 (2015) 1–18, https://doi.org/10.1111/tra.12230.
[6] T.A. Schulz, M.G. Choi, S. Raychaudhuri, J.A. Mears, R. Ghirlando, J.E. Hinshaw, W.A. Prinz, Lipid-regulated sterol transfer between closely apposed membranes by oxysterol-binding protein homologues, J. Cell Biol. 187 (2009) 889–903, https://doi.org/10.1083/jcb.200905007.
[7] T.P. Levine, S. Munro, The pleckstrin homology domain of oxysterol-binding protein recognizes a determinant specific to Golgi membranes, Curr. Biol. 8 (1998) 729–739, https://doi.org/10.1016/s0960-9822(98)70296-9.
[8] M. Lehto, S. Laitinen, G. Chinetti, M. Johansson, C. Ehnholm, B. Staels, E. Ikonen, V.M. Olkkonen, The OSBP-related protein family in humans, J. Lipid Res. 42 (2001) 1203–1213. https://www.ncbi.nlm.nih.gov/pubmed/11483621.
[9] B. Mesmin, B. Antonny, The counterflow transport of sterols and PI4P, Biochim. Biophys. Acta 1861 (2016) 940–951, https://doi.org/10.1016/j.bbalip.2016.02.024.
[10] B. Mesmin, J. Bigay, J. Moser von Filseck, S. Lacas-Gervais, G. Drin, B. Antonny, A four-step cycle driven by PI(4)P hydrolysis directs sterol/PI(4)P exchange by the ER-Golgi tether OSBP, Cell 155 (2013) 830–843, https://doi.org/10.1016/j.cell.2013.09.056.
[11] M. Lehto, J. Tienari, S. Lehtonen, E. Lehtonen, V.M. Olkkonen, Subfamily III of mammalian oxysterol-binding protein (OSBP) homologues: the expression and intracellular localization of ORP3, ORP6, and ORP7, Cell Tissue Res. 315 (2004) 39–57, https://doi.org/10.1007/s00441-003-0817-y.
[12] M. Ouimet, E.J. Hennessy, C. van Solingen, G.J. Koelwyn, M.A. Hussein, B. Ramkhelawon, K.J. Rayner, R.E. Temel, L. Perisic, U. Hedin, L. Maegdefessel, M. J. Garabedian, L.M. Holdt, D. Teupser, K.J. Moore, miRNA targeting of oxysterol-binding protein-like 6 regulates cholesterol trafficking and efflux, Arterioscler. Thromb. Vasc. Biol. 36 (2016) 942–951, https://doi.org/10.1161/ATVBAHA.116.307282.
[13] C. Herold, B.V. Hooli, K. Mullin, T. Liu, J.T. Roehr, M. Mattheisen, A.R. Parrado, L. Bertram, C. Lange, R.E. Tanzi, Family-based association analyses of imputed genotypes reveal genome-wide significant association of Alzheimer's disease with OSBPL6, PTPRG, and PDCL3, Mol. Psychiatr. 21 (2016) 1608–1612, https://doi.org/10.1038/mp.2015.218.
[14] E. Maestrini, A.T. Pagnamenta, J.A. Lamb, E. Bacchelli, N.H. Sykes, I. Sousa, C. Toma, G. Barnby, H. Butler, L. Winchester, T.S. Scerri, F. Minopoli, J. Reichert, G. Cai, J.D. Buxbaum, O. Korvatska, G.D. Schellenberg, G. Dawson, A. de Bildt, R. B. Minderaa, E.J. Mulder, A.P. Morris, A.J. Bailey, A.P. Monaco, IMGSAC High-density SNP association study and copy number variation analysis of the AUTS1 and AUTS5 loci implicate the IMMP2L-DOCK4 gene region in autism susceptibility, Mol. Psychiatr. 15 (2010) 954–968, https://doi.org/10.1038/mp.2009.34.
[15] S. Mochizuki, H. Miki, R. Zhou, Y. Kido, W. Nishimura, M. Kikuchi, Y. Noda, Oxysterol-binding protein-related protein (ORP) 6 localizes to the ER and ER-plasma membrane contact sites and is involved in the turnover of PI4P in cerebellar granule neurons, Exp. Cell Res. 370 (2018) 601–612, https://doi.org/10.1016/j.yexcr.2018.07.025.
[16] É. Sághy, M. Payrits, T. Bíró-Sütő, R. Skoda-Földes, E. Szánti-Pintér, J. Erostyák, G. Makkai, G. Sétáló, L. Kollár, T. Kőszegi, R. Csepregi, J. Szolcsányi, Z. Helyes, É. Szőke, Carboxamido steroids inhibit the opening properties of transient receptor potential ion channels by lipid raft modulation, J. Lipid Res. 59 (2018) 1851–1863, https://doi.org/10.1194/jlr.m084723.
[17] Y. Tashiro, T. Yamazaki, Y. Shimada, Y. Ohno-Iwashita, K. Okamoto, Axon-dominant localization of cell-surface cholesterol in cultured hippocampal neurons and its disappearance in Niemann-Pick type C model cells, Eur. J. Neurosci. 20 (2004) 2015–2021, https://doi.org/10.1111/j.1460-9568.2004.03677.x.
[18] K. Del Vecchio, R.V. Stahelin, Investigation of the phosphatidylserine binding properties of the lipid biosensor, Lactadherin C2 (Lact C2), in different membrane environments, J. Bioenerg. Biomembr. 50 (2018) 1–10, https://doi.org/10.1007/s10863-018-9745-0.
[19] H. Ye, B. Li, V. Subramanian, B.H. Choi, Y. Liang, A. Harikishore, G. Chakraborty, K. Baek, H.S. Yoon, NMR solution structure of C2 domain of MFG-E8 and insights into its molecular recognition with phosphatidylserine, Biochim. Biophys. Acta 1828 (2013) 1083–1093, https://doi.org/10.1016/j.bbamem.2012.12.009.
[20] J.G. Kay, M. Koivusalo, X. Ma, T. Wohland, S. Grinstein, Phosphatidylserine dynamics in cellular membranes, Mol. Biol. Cell 23 (2012) 2198–2212, https://doi.org/10.1091/mbc.e11-11-0936.

[21] P. INTRACELLULAR TRANSPORT J. Torta Chung, F. Masai, K. Lucast, L. Czapla, H. Tanner, L.B. Narayanaswamy, P. Wenk, M.R. Nakatsu, F. De Camilli, PI4P/phosphatidylserine countertransport at ORP5- and ORP8-mediated ER-plasma membrane contacts, Science 349 (2015) 428–432, https://doi.org/10.1126/science.aab1370.

[22] B. Antonny, J. Bigay, B. Mesmin, The oxysterol-binding protein cycle: burning off PI(4)P to transport cholesterol, Annu. Rev. Biochem. 87 (2018) 809–837, https://doi.org/10.1146/annurev-biochem-061516-044924.

[23] M. Sohn, P. Ivanova, H.A. Brown, D.J. Toth, P. Varnai, Y.J. Kim, T. Balla, Lenz-Majewski mutations in PTDSS1 affect phosphatidylinositol 4-phosphate metabolism at ER-PM and ER-Golgi junctions, Proc. Natl. Acad. Sci. U. S. A. 113 (2016) 4314–4319, https://doi.org/10.1073/pnas.1525719113.

[24] A. Alvarez-Prats, I. Bjelobaba, Z. Aldworth, T. Baba, D. Abebe, Y.J. Kim, S. S. Stojilkovic, M. Stopfer, T. Balla, Schwann-cell-specific deletion of phosphatidylinositol 4-kinase alpha causes aberrant myelination, Cell Rep. 23 (2018) 2881–2890, https://doi.org/10.1016/j.celrep.2018.05.019.

[25] N. Bojjireddy, J. Botyanszki, G. Hammond, D. Creech, R. Peterson, D.C. Kemp, M. Snead, R. Brown, A. Morrison, S. Wilson, S. Harrison, C. Moore, T. Balla, Pharmacological and genetic targeting of the PI4KA enzyme reveals its important role in maintaining plasma membrane phosphatidylinositol 4-phosphate and phosphatidylinositol 4,5-bisphosphate levels, J. Biol. Chem. 289 (2014) 6120–6132, https://doi.org/10.1074/jbc.m113.531426.

[26] G.R. Hammond, M.P. Machner, T. Balla, A novel probe for phosphatidylinositol 4-phosphate reveals multiple pools beyond the Golgi, J. Cell Biol. 205 (2014) 113–126, https://doi.org/10.1083/jcb.201312072.

[27] S.J. Stone, J.E. Vance, Phosphatidylserine synthase-1 and -2 are localized to mitochondria-associated membranes, J. Biol. Chem. 275 (2000) 34534–34540, https://doi.org/10.1074/jbc.m002865200.

[28] J.E. Vance, R. Steenbergen, Metabolism and functions of phosphatidylserine, Prog. Lipid Res. 44 (2005) 207–234, https://doi.org/10.1016/j.plipres.2005.05.001.

[29] T.M. Hughes, C. Rosano, R.W. Evans, L.H. Kuller, Brain cholesterol metabolism, oxysterols, and dementia, J. Alzheimers Dis. 33 (2013) 891–911, https://doi.org/10.3233/JAD-2012-121585.

[30] E.J. Gruber, A.Y. Aygun, C.A. Leifer, Macrophage uptake of oxidized and acetylated low-density lipoproteins and generation of reactive oxygen species are regulated by linear stiffness of the growth surface, PLoS One 16 (2021), e0260756, https://doi.org/10.1371/journal.pone.0260756.

[31] D. Yan, M.I. Mäyränpää, J. Wong, J. Perttilä, M. Lehto, M. Jauhiainen, P. T. Kovanen, C. Ehnholm, A.J. Brown, V.M. Olkkonen, OSBP-related protein 8 (ORP8) suppresses ABCA1 expression and cholesterol efflux from macrophages, J. Biol. Chem. 283 (2008) 332–340, https://doi.org/10.1074/jbc.M705313200.

[32] X. Gu, A. Li, S. Liu, L. Lin, S. Xu, P. Zhang, S. Li, X. Li, B. Tian, X. Zhu, X. Wang, MicroRNA124 regulated neurite elongation by targeting OSBP, Mol. Neurobiol. 53 (2016) 6388–6396, https://doi.org/10.1007/s12035-015-9540-4.

[33] A. Darbyson, J.K. Ngsee, Oxysterol-binding protein ORP3 rescues the Amyotrophic Lateral Sclerosis-linked mutant VAPB phenotype, Exp. Cell Res. 341 (2016) 18–31, https://doi.org/10.1016/j.yexcr.2016.01.013.